Mechanism of the Olefin Epoxidation Catalyzed by Molybdenum Diperoxo Complexes: Quantum-Chemical Calculations Give an Answer to a Long-Standing Question†

Dirk V. Deubel, Jörg Sundermeyer, and Gernot Frenking*

Contribution by the Fachbereich Chemie, Philipps-Universität Marburg, Hans-Meerwein-Strasse, D-35032 Marburg, Germany

Received February 23, 2000

Abstract: Quantum-chemical calculations at the B3LYP level have been carried out to elucidate the reaction mechanism of the epoxidation of ethylene with the molybdenum diperoxo complex $MoO(O_2)_2OPH_3$. All relevant transition states and intermediates which belong to the reaction pathways suggested by Mimoun and by Sharpless were optimized. The calculations show that there is no reaction channel from the ethylene complex to the putative metalla-2,3-dioxolane intermediate as suggested by Mimoun. There is a transition state for the direct formation of the five-membered cyclic intermediate from ethylene and the diperoxo complex. However, the subsequent extrusion of a C_2H_4O species from the metalla-2,3-dioxolane does not yield the epoxide but acetaldehyde. The calculations show that the reaction of $MoO(O_2)_2OPH_3$ with ethylene can directly lead to the epoxide as suggested by Sharpless. The activation energy for the latter process is 15.2 kcal/mol, which is lower than the barrier for the formation of the metalla-2,3-dioxolane (23.7 kcal/mol). Calculations with the ligand $OPMe_3$ instead of OPH_3 show an even larger preference of the pathway leading to the epoxide than the formation of the five-membered ring. The calculations strongly support the mechanism suggested by Sharpless, while the Mimoun mechanism leads to carbonyl compounds as reaction products. Examination of the electronic structure of the transition state of the epoxide formation with the Charge Decomposition Analysis shows that the reaction should be considered as nucleophilic attack of the olefin toward the σ^* orbital of the peroxo bond.

Introduction

Although numerous synthetic methods have been developed for the epoxidation of olefins, an industrial process for the oxidation of propylene yielding propylene oxide is still carried out on the million-ton-per-year scale by the expensive chlorohydrine process, despite the ecological problems which are associated with the reaction.[1] The well-established epoxidation via heterogeneous catalysis on silver surfaces cannot be used for propylene, because of the propensity of the allylic C−H bond for oxidation.[2] A possible solution for the chemoselectivity problem lies in the use of transition-metal (TM) compounds as homogeneous catalysts. Following the introduction of the Halcon−Arco process,[3] the focus of recent experimental studies has been on diperoxo complexes of group 5,[4] group 6,[5,6] and group 7[7] elements.

A promising method for the homogeneously catalyzed epoxidation with TM peroxides has recently been patented by BASF.[8] Sundermeyer and Wahl developed a process where the epoxidation is carried out in a two-phase reaction that is catalyzed by molybdenum peroxo complexes $[MoO(O_2)_2LL']$ ($L = OPR_3$, $R = n\text{-}C_{12}H_{25}$, $L' = H_2O$).[9] Molybdenum peroxo complexes with the formula $[MoO(O_2)_2LL']$ were first introduced as epoxidation catalysts with the ligands L = hmpa, L′ = H_2O in pioneering studies which were carried out by Mimoun.[10] The mechanism of the reaction, which is of outermost importance for a rational optimization of the process, has been the center of a decade-old unresolved controversy.[11]

The first suggestion about the mechanism of the stoichiometric epoxidation of olefins with $MoO(O_2)_2$(hmpa) was made

† Theoretical Studies of Organometallic Compounds. 41. Part 40: Chen. Y.; Petz, W.; Frenking, G. *Organometallics*, **2000**, *19*, 2698−2706.

(1) (a) Weissermel, K.; Arpe, H.-J. *Industrial Organic Chemistry*; Wiley-VCH: New York, 1997. (b) Sheldon, R. A. In *Applied Homogeneous Catalysis with Organometallic Compounds*; Cornils, B., Herrmann, W. A., Eds.; Wiley-VCH: Weinheim, 1996; Vol. 1, p 411.

(2) (a) Barteau, M. A.; Madix, R. J. In *The Chemical Physics of Solid Surfaces and Heterogeneous Catalysis*; King, D. A., Woodruff, D. P., Eds.; Elsevier: Amsterdam, 1982; p 85. (b) Van Santen, R. A.; Kuipers, H. P. C. E. *Adv. Catal.* **1987**, *35*, 265. (c) Satchler, W. M. H.; Backx, C.; Van Santen, R. A. *Catal. Rev.* **1981**, *23*, 127.

(3) Koller, J. U.S. Patent 3.350.422, 1967; U.S. Patent 3.351.635, 1967.

(4) (a) Butler, A.; Clague, M. J.; Meister, G. *Chem. Rev.* **1994**, *94*, 625 and literature cited therein. (b) Conte, V.; Di Furia, F.; Moro, S. *J. Mol. Catal.* **1997**, *120*, 93.

(5) (a) Neumann, R.; Cohen, M. *Angew. Chem.* **1997**, *109*, 1810; *Angew. Chem., Int. Ed. Engl.* **1997**, *36*, 1738. (b) Bösing, M.; Nöh, A.; Loose, I.; Krebs, B. *J. Am. Chem. Soc.* **1998**, *120*, 7252 and literature cited therein.

(6) Dickman, M. H.; Pope, M. T. *Chem. Rev.* **1994**, *94*, 569.

(7) (a) Romao, C. C.; Kühn, F. E.; Herrmann, W. A. *Chem. Rev.* **1997**, *97*, 3197 and literature cited therein. (b) Herrmann, W. A.; Fischer, R. W.; Marz, D. W. *Angew. Chem.* **1991**, *103*, 1706; *Angew. Chem., Int. Ed. Engl.* **1991**, *30*, 1638. (c) Herrmann, W. A.; Fischer, R. W.; Scherer, W.; Rauch, M. *Angew. Chem.* **1993**, *105*, 1209; *Angew. Chem., Int. Ed. Engl.* **1993**, *32*, 1157. (d) Adam, W.; Mitchell, C. M. *Eur. J. Org. Chem.* **1999**, 785. (e) Herrmann, W. A.; Marz, D. W.; Wagner, W.; Kuchler, J. G.; Weichselbaumer, G.; Fischer, R. W. (Hoechst AG) DE Patent 3.902.357, 1989; EP Patent 90101439.9, 1990.

(8) (a) Schulz, M.; Teles, J. H.; Sundermeyer, J.; Wahl, G. (BASF AG) DE Patent 195.33.31.4, 1995. (b) Schulz, M.; Teles, J. H.; Sundermeyer, J.; Wahl, G. (BASF AG) WO Patent 10054, 1995.

(9) Wahl, G.; Kleinhenz, D.; Schorm, A.; Sundermeyer, J.; Stowasser, R.; Rummey, C.; Bringmann, G.; Fickert, C.; Kiefer, W. *Chem. Eur. J.* **1999**, *5*, 3237.

(10) (a) Mimoun, H.; Seree de Roch, I.; Sajus, L. *Bull. Soc. Chem. Fr.* **1969**, 1481. (b) Mimoun, H.; Seree de Roch, I.; Sajus, L. *Tetrahedron* **1970**, *26*, 37.

(11) (a) Sundermeyer, J. *Angew. Chem.* **1993**, *105*, 1195; *Angew. Chem., Int. Ed. Engl.* **1993**, *32*, 1144. (b) Jørgensen, K. A. *Chem. Rev.* **1989**, *89*, 431.

10.1021/ja0006649 CCC: $19.00
Published on Web 10/03/2000

Scheme 1. Schematic Representation of the Reaction Mechanisms Suggested by Mimoun (top) and by Sharpless (bottom)

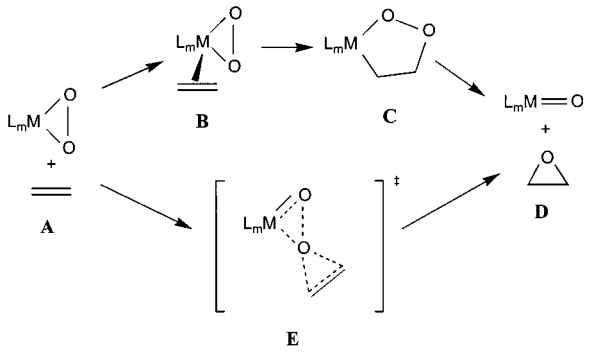

by Mimoun.[10b] The author interpreted his kinetic investigations in favor of a multiple-step process that is shown in Scheme 1. According to Mimoun, the first step of the reaction involves a coordination of the olefin to the metal yielding the olefin complex **B** as putative intermediate. The second step is a cycloinsertion of the olefin into one molybdenum−peroxo bond which leads to the metalla-2,3-dioxolane **C**. Examples for such metallacyclic compounds could later become isolated, but only for late transition metals.[12] The third step of the Mimoun mechanism is the cycloextrusion of the olefin which gives the TM oxide that further reacts with H_2O_2 yielding the peroxo complex in a catalytic cycle.[13] We want to point out that the first step of the Mimoun mechanism may proceed via two different paths. Mimoun favored substitution of the phosphine oxide by the olefin,[14] while Arakawa suggested the addition of the olefin.[15]

An alternative mechanism for the epoxidation reaction with molybdenum peroxo complexes has later been introduced by Sharpless.[16] The author suggested that the reaction takes place in a concerted way via transition state **E** (Scheme 1) where the olefin attacks an oxygen atom of a peroxo group. The controversy whether the epoxidation reaction takes place as a three-step reaction via **B** and **C** (Mimoun mechanism) or as a concerted reaction via transition state **E** (Sharpless mechanism) has not been solved until now, although numerous experimental[17] and theoretical[18] efforts were made which address the question. A recent kinetic study of the catalytic epoxidation reaction with alkylhydroperoxide by Thiel et al.[19] revealed interesting information about the mechanism. However, the experiments were carried out with *tert*-butylhydroperoxide as oxidant which can coordinate to the metal. The results may therefore not be applied to the much more difficult catalytic activation of hydrogen peroxide for the epoxidation in a two-phase system. Rösch et al. have recently performed DFT studies of the epoxidation of olefins with rhenium[20] and titanium[21] compounds. The rhenium-catalyzed epoxidation has also been investigated theoretically by Wu and Sun.[22] The theoretical[20,22] work and kinetic studies by Espenson[23] suggest that the epoxidation with rhenium oxodiperoxo complexes probably follows the Sharpless mechanism. The effect of ligands on the latter reaction was recently investigated by Rösch.[24] The results are important but may not carry over to the reaction using molybdenum compounds.

The unresolved controversy about the two reaction mechanisms of the epoxidation reaction which are shown in Scheme 1 resembles the situation which existed until recently for the dihydroxylation of olefins with OsO_4. The long-standing debate whether the reaction takes place as a two-step pathway via initial [2+2] addition followed by ring expansion[25] or via a concerted [3+2] addition[26] was finally ended by quantum-chemical calculations which showed that the concerted reaction has a much lower activation barrier than the two-step mechanism.[27] The calculated result was later supported by experimental and theoretical studies of kinetic isotope effects which are in agreement with a concerted pathway.[28]

Recently we calculated the reaction energies of the reaction of MoO_3 with H_2O_2 yielding the peroxo compounds $MoO_n(O_2)_{3-n}$ and the energies of the epoxidation reaction of ethylene with $[MoO_n(O_2)_{3-n}LL']$ with and without the ligands $L = OPH_3$ and $L' = H_2O$.[29] The results of this work clearly show that the molybdenum diperoxo complexes are thermodynamically favored over the monoperoxo and triperoxo complexes. This explains the peculiar stability of neutral[30] molybdenum complexes with two peroxo groups relative to monoperoxo and triperoxo complexes. Diperoxo complexes of molybdenum have been characterized by X-ray structure analysis[31] while experi-

(12) (a) Mimoun, H. *Pure Appl. Chem.* **1981**, *53*, 2389. (b) Sheldon, R. A.; Van Doorn, J. A. *J. Organomet. Chem.* **1975**, *94*, 115. (c) Ugo, R. *Engelhard Ind. Tech. Bull.* **1971**, *11*, 45. (d) Broadhurst, M. J.; Brown, J. M.; John. R. A. *Angew. Chem.* **1983**, *95*, 57; *Angew. Chem., Int. Ed. Engl.* **1983**, *22*, 47.

(13) It has been shown that the reaction of the molybdenum oxide complex with H_2O_2 yielding the peroxide is not an oxidation reaction but rather a perhydrolysis. The oxo group is substituted in an addition−elimination reaction by the peroxo group of the peroxide: Faller, J. W.; Ma, Y. *J. Organomet. Chem.* **1989**, *368*, 45.

(14) Mimoun, H. *Angew. Chem.* **1982**, *94*, 750; *Angew. Chem., Int. Ed. Engl.* **1982**, *21*, 734.

(15) Arakawa, H.; Moro-Oka, Y.; Ozaki, A. *Bull. Chem. Soc. Jpn.* **1974**, *47*, 2958.

(16) Sharpless, K. B.; Townsend, J. M.; Williams, D. R. *J. Am. Chem. Soc.* **1972**, *94*, 295.

(17) (a) Arcoria, A.; Ballistreri, F. P.; Tomaselli, G. A.; Di Furia, F.; Modena, G. *J. Mol. Catal.* **1983**, *18*, 177. (b) Jacobson, S. E.; Muccigrosso, D. A.; Mares, F. *J. Org. Chem.* **1979**, *14*, 921. (c) Amato, G.; Arcoria, A.; Ballistreri, F. P.; Tomaselli, G. A. *J. Mol. Catal.* **1986**, *37*, 165. (d) Talsi, E. P.; Shalyaev, K. V.; Zamaraev, K. I. *J. Mol. Catal.* **1993**, *83*, 347.

(18) Bach, R. D.; Wolber, G. J.; Coddens, B. A. *J. Am. Chem. Soc.* **1984**, *106*, 6098. (b) Jørgensen, J. A.; Hoffmann, R. *Acta Chem. Scand. B* **1986**, *40*, 411. (c) Salles, L.; Piquemal, J.-Y.; Thouvenot, R.; Minot, C.; Brégeault, J.-M. *J. Mol. Catal. A* **1997**, *117*, 375.

(19) (a) Thiel, W. R.; Priermeyer, T. *Angew. Chem.* **1995**, *107*, 1870; *Angew. Chem., Int. Ed. Engl.* **1995**, *34*, 1737. (b) Thiel, W. R. *Chem. Ber.* **1996**, *129*, 575. (c) Thiel, W. R. *J. Mol. Catal. A* **1997**, *117*, 449. (d) Thiel, W. R.; Eppinger, J. *Chem. Eur. J.* **1997**, *3*, 696.

(20) Gisdakis, P.; Antonczak, S.; Köstlmeier, S.; Herrmann, W. A.; Rösch, N. *Angew. Chem.* **1998**, *110*, 2333; *Angew. Chem., Int. Ed. Engl.* **1998**, *37*, 2211.

(21) Yudanov, I. V.; Gisdakis, P.; Di Valentin, C.; Rösch, N. *Eur. J. Inorg. Chem.* **1999**, *5*, 3603.

(22) Wu, Y. D.; Sun, J. *J. Org. Chem.* **1998**, *63*, 1752.

(23) (a) Al-Aljouni, A. M.; Espenson, J. H. *J. Am. Chem. Soc.* **1995**, *117*, 9243. (b) Al-Aljouni, A. M.; Espenson, J. H. *J. Org. Chem.* **1996**, *61*, 3969. (c) Tan, H.; Espenson, J. H. *Inorg. Chem.* **1998**, *37*, 467.

(24) Kühn, F. E.; Santos, A. M.; Roesky, P. W.; Herdtweck, E.; Scherer, S.; Gisdakis, P.; Yudanov, I. V.; Di Valentin, C.; Rösch, N. *Chem. Eur. J.* **1999**, *5*, 3603.

(25) Sharpless, K. B.; Teranishi, A. Y.; Bäckvall, J.-E. *J. Am. Chem. Soc.* **1977**, *99*, 3120.

(26) (a) Criegee, R.; Marchand, B.; Wannowius, H. *Liebigs Ann. Chem.* **1942**, *550*, 99. (b) Corey, E. J.; Jardine, P. D.; Virgil, S.; Yuen, P.-W.; Connell, R. D. *J. Am. Chem. Soc.* **1989**, *111*, 9243.

(27) (a) Pidun, U.; Boehme, C.; Frenking, G. *Angew. Chem.* **1996**, *108*, 3008; *Angew. Chem., Int. Ed. Engl.* **1996**, *35*, 2817. (b) Dapprich, S.; Ujaque, G.; Maseras, F.; Lledós, A.; Musaev, D. G.; Morokuma, K. *J. Am. Chem. Soc.* **1996**, *118*, 11660. (c) Torrent, M.; Deng, L.; Duran, M.; Sola, M.; Ziegler, T. *Organometallics* **1997**, *16*, 13.

(28) Del Monte, A. J.; Haller, J.; Houk, K. N.; Sharpless, K. B.; Singleton, D. A.; Strassner, T.; Thomas, A. A. *J. Am. Chem. Soc.* **1997**, *119*, 9907.

(29) Deubel, D. V.; Sundermeyer, J.; Frenking, G. *Inorg. Chem.* **2000**, *39*, 2314.

(30) Anionic tri- and tetraperoxo complexes of molybdenum have been observed in basic solution: (a) Nardello, V.; Marko, J.; Vermeersch, G.; Aubry, J. M. *Inorg. Chem.* **1995**, *34*, 4950. (b) Aubry, J. M.; Bouttemy, S. *J. Am. Chem. Soc.* **1997**, *119*, 5286. (c) Nardello, V.; Marko, J.; Vermeersch, G.; Aubry, J. M. *Inorg. Chem.* **1998**, *37*, 5418.

mental geometries of complexes with one or three peroxo groups are not known. The mechanism of the epoxidation was not investigated in our previous work. Here we report the first quantitative theoretical study on the mechanism of the Mo-catalyzed epoxidation reaction. Previous theoretical studies used EHT calculations which can only be considered as qualitative work.[11b,46] We give the first quantum chemical investigation of the complete reaction pathways which were postulated by Mimoun[10b] and by Sharpless[16] using $[MoO(O_2)_2(OPH_3)]$ and $[MoO(O_2)_2(OPMe_3)]$ as model catalysts. We also calculated other possible reaction steps of the epoxidation process which will be discussed below. The results of this work give a clear answer to the question whether the Mimoun mechanism or the Sharpless mechanism should be considered as the correct description of the epoxidation of olefins with molybdenum diperoxo complexes.

Methods

The calculations have been carried out at the B3LYP[32] level of theory with two different basis sets. For the geometry optimizations and frequency calculations we used our standard basis set II[33] which has a quasi-relativistic small-core ECP[34] with a (441/2111/31) valence basis set at Mo and 6-31G(d) basis sets at the other atoms. Optimized structures have been identified as energy minima or transition states by calculation of the eigenvalues of the Hessian matrices. The zero-point vibrational energies (ZPE) are not scaled. Calculations of the intrinsic reaction path (IRC)[35] were carried out at B3LYP/II using the optimized transition states as starting points to find out the respective educts and products. Single-point energy calculations were carried out at the B3LYP level by using the larger basis set combination III+ at B3LYP/II optimized geometries. Basis set III+ has the same ECP[34] for Mo as basis set II but the basis functions are completely uncontracted and augmented by a set of f-type polarization functions[36] with the coefficient $\zeta = 1.043$, while 6-31+G(d) basis sets were employed for the other atoms. Recent calculations of metal−oxide additions to olefins have shown that calculated energies at B3LYP/III+ are in very good agreement with experimental values and with theoretical energies which are obtained at the CCSD(T) level.[37] The calculations have been carried out with the program packages Gaussian 94 and Gaussian 98.[38] The interactions between the molybdenum diperoxide complex and ethylene were investigated with the charge decomposition analysis (CDA)[39] which has proven to be very helpful for gaining insight into transition metal−ligand interactions.[40] The CDA calculations were performed with the program CDA 2.1.[41]

Results and Discussion

The reaction courses given in Scheme 1 show the two mechanisms that were suggested by Mimoun[10b] and by Sharpless.[16] In the course of our investigations we also considered two alternative pathways which are related to the Mimoun mechanism. They are shown in Scheme 2, which also gives the numbers that are used in our work for the intermediates and the transition states. One alternative pathway of the Mimoun mechanism is the direct formation of the metalla-2,3-dioxolane **3** from the model catalyst $[MoO(O_2)_2(OPH_3)]$ (**1**) and ethylene via transition state **TS8**. The other alternative is the direct formation of the epoxide from the olefin diperoxo complex **2** via **TS6**. Both reaction steps, which have not been considered before, may be regarded as shortcuts of the Mimoun mechanism.

Thermodynamic Reaction Profile. We first calculated the reaction energies of the reaction steps according to the Mimoun mechanism (Scheme 2) $\mathbf{1} + C_2H_4 \rightarrow \mathbf{2} \rightarrow \mathbf{3} \rightarrow \mathbf{4} + C_2H_4O$. We also calculated the energies of the related species which do not have a OPH_3 ligand. This gives the thermodynamic reaction profile for the reaction $\mathbf{1^*} + C_2H_4 \rightarrow \mathbf{2^*} \rightarrow \mathbf{3^*} \rightarrow \mathbf{4^*} + C_2H_4O$, where the asterisk indicates that the OPH_3 ligand is missing. The optimized geometries are shown in Figure 1. The calculated energies are given in the Supporting Information. Figure 2 shows the theoretically predicted thermodynamic reaction profile of the Mimoun mechanism.

The calculations predict that the overall reaction $\mathbf{1} + C_2H_4 \rightarrow \mathbf{4} + C_2H_4O$ is exothermic by −35.2 kcal/mol, which indicates that the Mimoun mechanism is thermodynamically feasible. There is no experimental value available that can be compared to the calculated result. The formation of the olefin complex **2** is slightly endothermic. This has been discussed before.[29] It is noteworthy that the ethylene complex **2** is a true minimum, while diperoxo complexes of Re(VII) with ethylene ligands are not minima on the potential energy surface.[20] The subsequent formation of the metalla-2,3-dioxolane isomer **3a** is slightly exothermic with regard to **1** + ethylene by −2.5 kcal/mol (−7.9 kcal/mol with regard to **2**). The complex **3a**, which has the OPH_3 ligand trans to the Mo−C bond, is significantly more stable by 10.8 kcal/mol than the isomeric form **3b**.

(31) The X-ray structure analysis of $[MoO(O_2)_2(hmpa)(H_2O)]$ has been reported in: Le Carpentier, J.-M.; Schlupp, R.; Weiss, R. *Acta Crystallogr.* **1972**, *B28*, 1278.

(32) (a) Becke, A. D. *J. Chem. Phys.* **1993**, *98*, 5648. (b) Lee, C.; Yang, W.; Parr, R. G. *Phys. Rev. B* **1988**, *37*, 785. (c) Stevens, P. J.; Devlin, F. J.; Chablowski, C. F.; Frisch, M. J. *J. Phys. Chem.* **1994**, *98*, 11623.

(33) Frenking, G.; Antes, I.; Boehme, M.; Dapprich, S.; Ehlers, A. W.; Jonas, V.; Neuhaus, A.; Otto, M.; Stegmann, R.; Veldkamp, A.; Vyboishchikov, S. F. *Reviews in Computational Chemistry*; Lipkowitz, K. B., Boyd, D. B., Eds.; VCH: New York, **1996**; Vol. 8, pp 63−144.

(34) Hay, P. J.; Wadt, W. R. *J. Chem. Phys.* **1985**, *82*, 299.

(35) Fukui, K. *Acc. Chem. Res.* **1981**, *14*, 363.

(36) Ehlers, A. W.; Böhme, M.; Dapprich, S.; Gobbi, A.; Höllwarth, A.; Jonas, V.; Köhler, K. F.; Stegmann, R.; Veldkamp, A.; Frenking, G. *Chem. Phys. Lett.* **1993**, *208*, 111.

(37) Deubel, D. V.; Frenking, G. *J. Am. Chem. Soc.* **1999**, *121*, 2021.

(38) (a) Gaussian 94: Frisch, M. J.; Trucks, G. W.; Schlegel, H. B.; Gill, P. M. W.; Johnson, B. G.; Robb, M. A.; Cheeseman, J. R.; Keith, T. A.; Petersson, G. A.; Montgomery, J. A.; Raghavachari, K.; Al-Laham, M. A.; Zakrzewski, V. G.; Ortiz, J. V.; Foresman, J. B.; Cioslowski, J.; Stefanov, B. B.; Nanayakkara, A.; Challacombe, M.; Peng, C. Y.; Ayala, P. Y.; Chen, W.; Wong, M. W.; Andres, J. L.; Replogle, E. S.; Gomberts, R.; Martin, R. L.; Fox, D. J.; Binkley, J. S.; Defrees, D. J.; Baker, I.; Stewart, J. J. P.; Head-Gordon, M.; Gonzalez, C.; Pople, J. A. Gaussian Inc.: Pittsburgh, PA, 1995. (b) Gaussian 98 (Revision A.1): Frisch, M. J.; Trucks, G. W.; Schlegel, H. B.; Scuseria, G. E.; Robb, M. A.; Cheeseman, J. R.; Zakrzewski, V. G.; Montgomery, J. A.; Stratmann, R. E.; Burant, J. C.; Dapprich. S.; Milliam, J. M.; Daniels, A. D.; Kudin, K. N.; Strain, M. C.; Farkas, O.; Tomasi, J.; Barone, V.; Cossi, M.; Cammi, R.; Mennucci, B.; Pomelli, C.; Adamo, C.; Clifford, S.; Ochterski, J.; Petersson, G. A.; Ayala, P. Y.; Cui, Q.; Morokuma, K.; Malick, D. K.; Rabuck, A. D.; Raghavachari, K.; Foresman, J. B.; Cioslowski, J.; Ortiz, J. V.; Stefanov, B. B.; Liu, G.; Liashenko, A.; Piskorz, P.; Komaromi, I.; Gomberts, R.; Martin, R. L.; Fox, D. J.; Keith, T. A.; Al-Laham, M. A.; Peng, C. Y.; Nanayakkara, A.; Gonzalez, C.; Challacombe, M.; Gill, P. M. W.; Johnson, B. G.; Chen, W.; Wong, M. W.; Andres, J. L.; Head-Gordon, M.; Replogle, E. S.; Pople, J. A. Gaussian Inc.: Pittsburgh, PA, 1998.

(39) Dapprich, S.; Frenking, G. *J. Phys. Chem.* **1995**, *99*, 9352.

(40) (a) Pidun, U.; Frenking, G. *Organometallics* **1995**, *14*, 5325. (b) Frenking, G.; Pidun, U. *J. Chem. Soc., Dalton Trans.* **1997**, 1653. (c) Vyboishchikov, S. F.; Frenking, G. *Chem. Eur. J.* **1998**, *4*, 1428. (d) Vyboishchikov, S. F.; Frenking, G. *Chem. Eur. J.* **1998**, *4*, 1439.

(41) CDA 2.1, Dapprich, S.; Frenking, G. Marburg, 1994. The program is available via anonymous ftp server: ftp.chemie.uni-marburg.de/pub/cda.

(42) Mimoun, H.; Perez-Machirant, M. M.; Seree de Roch, I. *J. Am. Chem. Soc.* **1978**, *100*, 5437.

(43) (a) Herges, R. *Angew. Chem.* **1994**, *106*, 261; *Angew. Chem., Int. Ed. Engl.* **1994**, *33*, 255. (b) Herges, R. *J. Chem. Inf. Comput. Sci.* **1994**, *34*, 91.

(44) (a) Bach, R. D.; Owensby, A. L.; Andres, J. L.; Schlegel, H. B. *J. Am. Chem. Soc.* **1991**, *113*, 7031. (b) Bach, R. D.; Andres, J. L.; Owensby, A. L.; Schlegel, H. B.; McDouall, J. J. W. *J. Am. Chem. Soc.* **1992**, *114*, 7207. (c) Houk, K. N.; Liu, J.; DeMello, N. C.; Condroski, K. R. *J. Am. Chem. Soc.* **1997**, *119*, 10147. (d) Jenson, C.; Liu, J.; Houk, K. N.; Jorgensen, W. L. *J. Am. Chem. Soc.* **1997**, *119*, 12982. (e) Liu, J.; Houk, K. N. *J. Org. Chem.* **1998**, *63*, 8565. (f) Adam, W.; Curci, R.; D'Accolti, L.; Dinoi, A.; Fusco, C.; Gasparrini, F.; Kluge, R.; Paredes, R.; Schulz, M.; Smerz, A. K.; Veloza, L. A.; Weinkötz, S.; Winde, R. *Chem. Eur. J.* **1997**, *3*, 105.

(45) Herrmann, W. A.; Fischer, R. W.; Scherer, W.; Rauch, M. U. *Angew. Chem.* **1993**, *105*, 1209; *Angew. Chem., Int. Ed. Engl.* **1993**, *32*, 1157.

(46) Purcell, K. F. *Organometallics* **1985**, *4*, 509.

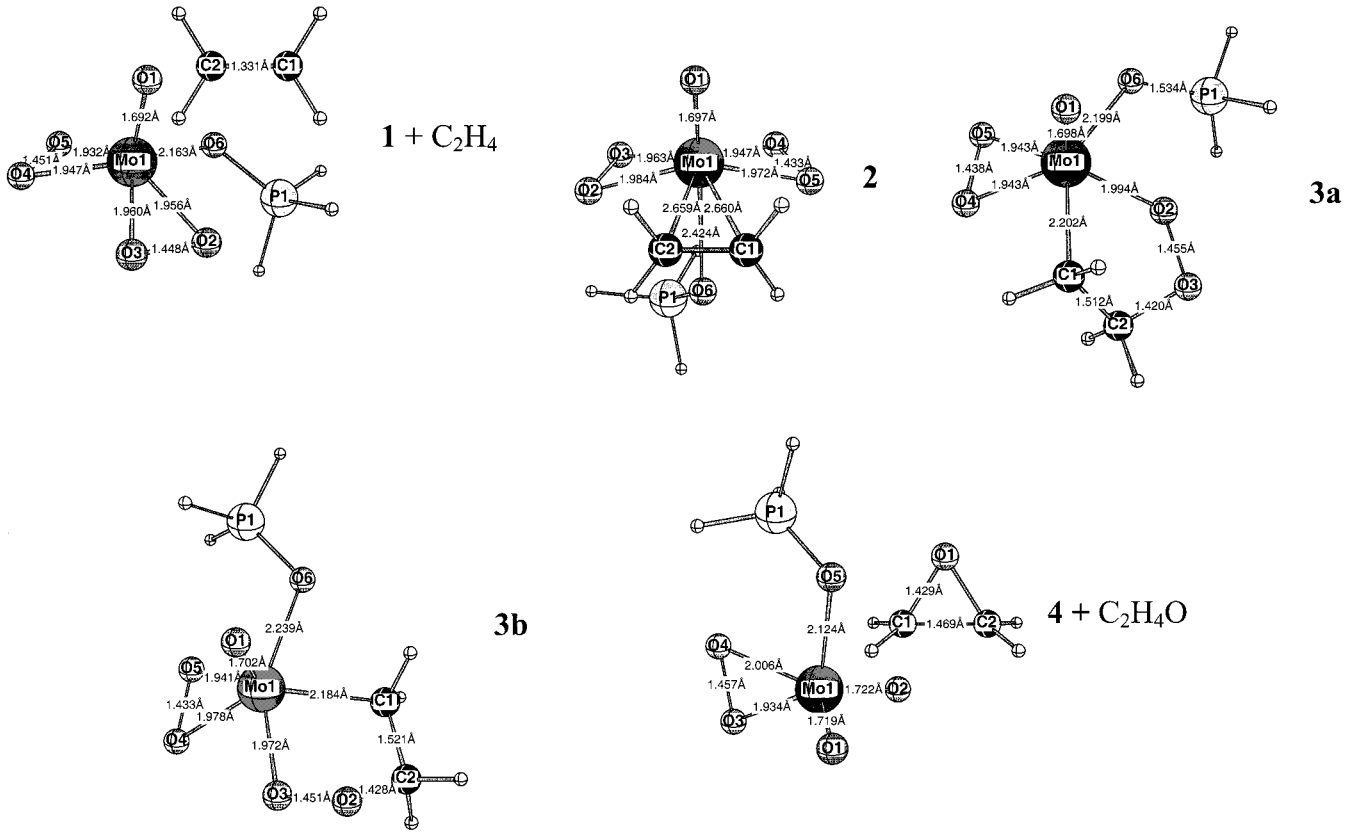

Figure 1. Optimized energy minima at B3LYP/II. Distances are given in Å.

Scheme 2. Schematic Representation of the Energy Minima and Transition States of the Epoxidation Reaction Which Have Been Investigated in Our Work

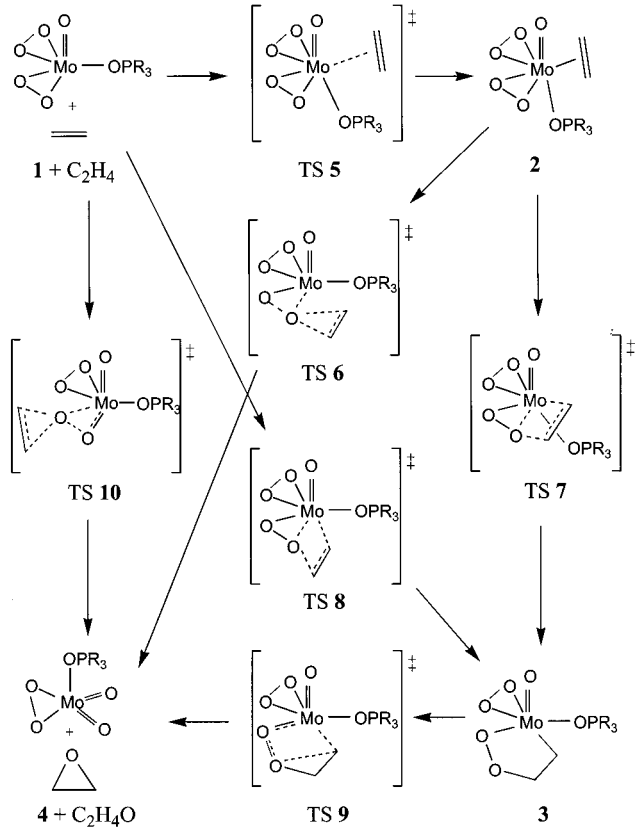

Figure 2 shows that the epoxidation reaction with the molybdenum complex **1** which has a phosphine oxide ligand is

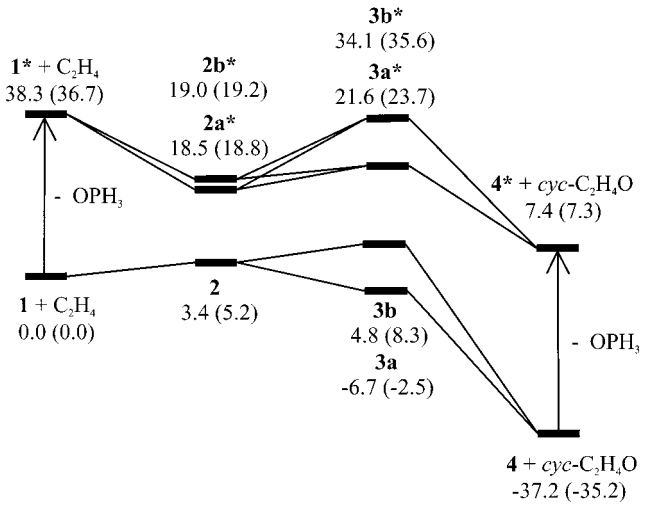

Figure 2. Thermodynamic reaction profile of the Mimoun mechanism with (bottom) and without (top) the OPH_3 ligand. An asterisk denotes the complex without the PH_3 ligand. Calculated energies at B3LYP/III+//B3LYP/II in kcal/mol. ZPE-corrected values are given in parentheses.

exothermic by −35.2 kcal/mol. The reaction without the OPH_3 ligand **1*** + C_2H_4 → **4*** + C_2H_4O is exothermic by −29.4 kcal/mol. The main difference between the two pathways is the reaction energies for the formation of the olefin complexes. The first step of the reaction in the presence of OPH_3 is endothermic, while the first step of the reaction without OPH_3 is strongly exothermic by −17.9 kcal/mol. This is because ethylene binds much stronger to the "naked" peroxo complex **1*** than to **1** where OPH_3 is already bound to the metal. Although the overall reaction course of the reaction without the OPH_3 ligand is also thermodynamically feasable, we do not think that it plays a role in the reaction course. Figure 2 shows that all intermediates

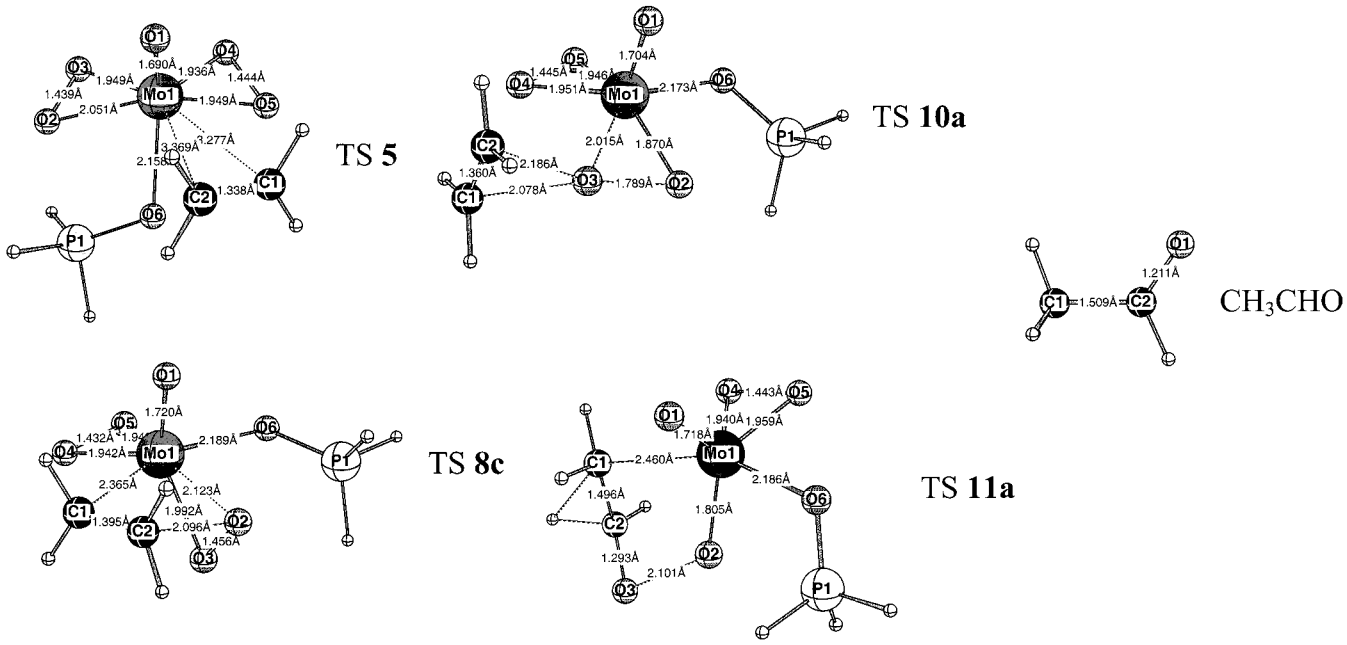

Figure 3. Optimized transiton states at B3LYP/II. Distances are given in Å.

Table 1. Calculated Relative Energies E_{rel} (B3LYP/III+//B3LYP/II) [kcal/mol] for Ethylene Epoxidation with Mimoun-Type Diperoxo Complexes $[MnO(O_2)_2(OPR_3)]$ (R = H (**1**), CH_3 (**1Me**)) with ZPE-Corrected Values (B3LYP/II) Given in Parentheses

	E_{rel}			
molecule/transition state	R = H		R = CH_3	
$[MoO(O_2)_2(OPR_3)] + C_2H_4$	**1** + C_2H_4	0.0 (0.0)	**1Me** + C_2H_4	0.0 (0.0)
$[MoO(O_2)_2(OPR_3)(C_2H_4)]$	**2**	3.4 (5.2)	**2Me**	9.1 (10.7)
$MoO(O_2)$-2,3-dioxolane	**3a**	−6.7 (−2.5)	**3aMe**	−2.4 (1.3)
	3b	4.8 (8.3)		
$[MoO_2(O_2)(OPR_3)] + C_2H_4O$	**4** + C_2H_4O	−37.2 (−35.2)	**4Me** + C_2H_4O	−38.0 (−36.0)
TS C_2H_4 addition	TS **5**	5.6 (6.9)	TS **5Me**	10.9 (11.7)
TS subsequent oxirane formation	TS **6**	*a*		
TS subsequent cycloinsertion	TS **7**	*a*		
TS direct cycloinsertion	TS **8a**	23.7 (25.7)		
	TS **8b**	29.6 (32.1)		
	TS **8c**	21.5 (23.7)	TS **8cMe**	26.8 (28.4)
	TS **8d**	23.0 (24.9)		
	TS **8e**	32.3 (34.4)		
	TS **8f**	35.9 (38.0)		
TS cycloextrusion of oxirane	TS **9**	*a*		
TS direct oxirane formation	TS **10a**	14.2 (15.2)	TS **10aMe**	16.6 (17.5)
	TS **10b**	23.8 (24.7)		
TS aldehyde formation	TS **11a**	16.3 (16.9)	TS **11aMe**	18.9 (19.3)
	TS **11b**	35.1 (35.8)		
$[MoO_2(O_2)(OPR_3)] + CH_3CHO$	**4** + CH_3CHO	−65.1 (−64.2)	**4Me** + CH_3CHO	−65.9 (−65.0)

[a] No transition state found.

without an OPH_3 ligand remain much higher in energy than the OPH_3 complexed species. Therefore, we restricted our kinetic investigations on the species which are shown in Scheme 2.

Kinetic Reaction Profile. The optimized geometries of the transition states are shown in Figure 3. The calculated energies are given in Table 1.

We begin the discussion with the kinetic energy profile of the Mimoun mechanism. The first step of the reaction pathway is the formation of the olefin complex **2**. There is only a small barrier that separates the educts **1** + C_2H_4 from **2**. The activation energy for the forward reaction is 6.9 kcal/mol and the barrier for loss of ethylene is only 1.7 kcal/mol. The calculated energies indicate that there might be an equilibrium between **1** and **2**, from which the metalla-2,3-dioxolane **3** could be formed as suggested by Mimoun. We searched for a transition state **TS7** for the rearrangment **2** → **3**. Despite intensive efforts using numerous starting geometries and optimization procedures we were unable to locate **TS7** on the potential energy surface. We also could not find a transition state **TS6** that directly leads from the olefin complex to the epoxide (Scheme 2). The optimization always led to reaction channels where the ethylene ligand dissociates. This is not surprising considering the small activation barrier for the dissociation reaction **2** → **1** + C_2H_4. The calculations indicate that the olefin complex **2** is a dead-end street in the reaction cycle and not an intermediate which leads to the epoxide. Even if it is formed it should not play a role in the reaction mechanism.

We succeeded, however, in finding a transition state **TS8** for the direct formation of **3** from the starting material **1** + C_2H_4. In fact we found *six* different transition states **TS8a**−**TS8f** for the reaction. This comes from the fact that the attack of the olefin toward a Mo−peroxo bond can occur from different sides. This is schematically shown in Scheme 3. The attack can occur

Scheme 3. Schematic Representation of the Six Pathways for the Insertion Reaction of Ethylene into the Mo−O Bond of the Peroxo Ligands Leading to **TS8a**−**TS8f**

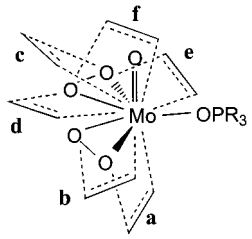

Scheme 4. Theoretically Predicted Pathway of the Decomposition Reaction of the Metalla-2,3-dioxolane **3**

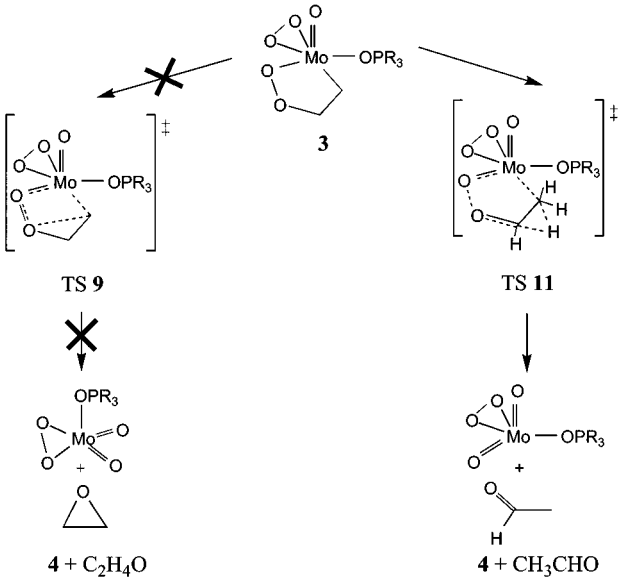

from a direction that is trans to the Mo=O bond (**a** and **b**) or it can take place from a cis position. This leads to four transition state **c**−**f**. The transition state **TS8c** shown in Figure 3 is the energetically lowest lying form. The geometries of the other transition states **TS8a**, **TS8b**, and **TS8d**−**f** are given as Supporting Information. The transition states **TS8b**−**d** lead to the energetically lower lying isomer **3a**, while the other transition states lead to **3b**. Thus, the calculations predict that the starting material **1** + C_2H_4 can directly yield the metalla-2,3-dioxolane **3a** via **TS8c** with an activation barrier of 23.7 kcal/mol.

The final step of the Mimoun mechanism is the extrusion of the epoxide from **3** (Scheme 2). The search for a transition state **TS9** led to a structure with one imaginary frequency which is only 16.9 kcal/mol above the starting compounds **1** + C_2H_4. Calculation of the IRC showed, however, that the transition state does not lead to ethylene epoxide but rather to acetaldehyde. This is schematically shown in Scheme 4. Since this is a different reaction channel we numbered the transition state as **11a**. Figure 3 shows that the geometry of **11a** clearly indicates a synchronous process where one hydrogen atom migrates from C2 to C1 while the C1−Mo1 and particularly the O2−O3 bonds are much longer than in **3a**, which shows the extrusion of the ligand. **TS11a** is the transition state for the extrusion of acetaldehyde from **3a**. A second transition state **11b** which connects the higher lying isomer **3b** with acetaldehye and **4** is much higher in energy (Table 1). The geometry of **TS11b** is given in the Supporting Information.

The calculations suggest that the mechanism suggested by Mimoun for the reaction of olefins with **1** does *not* give an epoxide but instead an aldehyde. Metalla-2,3-dioxolanes of later

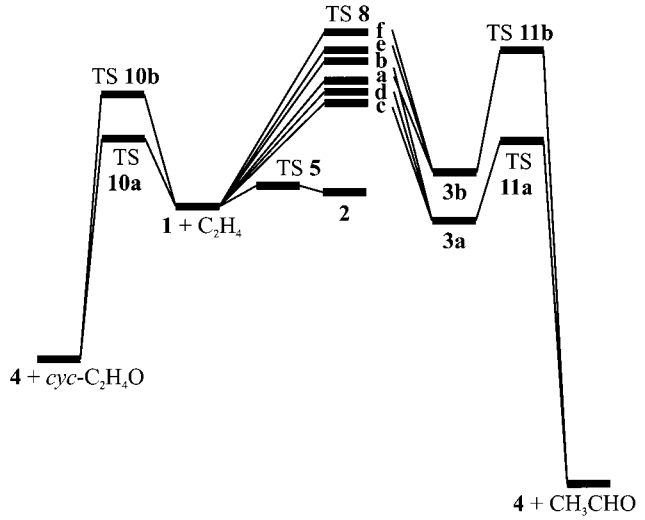

Figure 4. Theoretically predicted reaction profile of the epoxidation reaction showing the activation barriers **TS5**, **TS8**, and **TS11**, which are relevant for the Mimoun mechanism, and **TS10**, which refers to the Sharpless mechanism.

TMs have been isolated[12] and their thermic reactivity has been studied. It was found that they either react under sigmatropic cycloreversion yielding the carbonyl compound[42] or that C−C bond breaking of the olefin is observed.[12b] Our results suggest that *the thermal reactions of molybdenum-2,3-dioxolanes also do not give epoxides but carbonyl compounds as products*.

Now we discuss the Sharpless mechanism. Searching for the transition state of the reaction **1** + C_2H_4 → **4** + *c*-CH_2CH_2O led to two transition structures **TS10a** and **TS10b**. IRC calculations proved that **TS10a** and **TS10b** are indeed the transition states of the Sharpless mechanism. The geometry of **TS10a** (Figure 3) reveals an attack of the olefin to the oxygen atom O3 which is pointing away from the OPH_3 ligand, while in **TS10b** (Figure Sup1) the attack occurs toward the oxygen atom O2. **TS10a** is 9.5 kcal/mol lower in energy than **TS10b** (Table 1). A comparison of the geometries of **TS10a** and the educt complex **1** (Figure 1) shows that the olefin attacks the longest and presumably weakest Mo−peroxo bond. The carbon−oxygen distances in **TS10a** reveal that the C−O bond formation of the epoxide takes place in an asynchroneous fashion (Figure 3). The value for C1−O3 is clearly shorter (2.078 Å) than the C2−O3 interatomic distance (2.186 Å). The O2−O3 bond of the reacting peroxo group is significantly stretched in **TS10a** (1.789 Å) compared with that in the diperoxo complex **1** (1.451 Å), while the C−C distance of ethylene is only slightly longer (1.360 Å) in **TS10a** than in the free species (1.331 Å). The calculated energy of **TS10a** gives a theoretically predicted activation barrier for the epoxidation reaction of the parent system **1** + C_2H_4 of 15.2 kcal/mol. We want to point out that **TS10a** and **TS10b** have a spiro structure where the two planes Mo1−O2−O3 and C1−C2−O2/3 are orthogonal to each other. Thus, the molybdenum-catalyzed epoxidation via **TS10** can topologically be classified as a [2+1+2] coarctate reaction following the notation of Herges,[43] which can therefore be considered as the metalla analogue to the epoxidation of olefins with dioxiranes.[44]

Figure 4 shows the calculated reaction profile of the epoxidation reaction according to the Sharpless and the Mimoun mechanism. The latter pathway via **TS5** to the olefin complex **2** has a dead-end. The energetically lowest lying pathway to the more stable isomer of the metalla-2,3-dioxolane **3a** has an activation barrier of 23.7 kcal/mol for **TS8c**. The extrusion of

Scheme 5. Schematic Represenation of the Calculated Transition States of the Epoxidation of Ethylene with the Monoperoxo Complex **4**

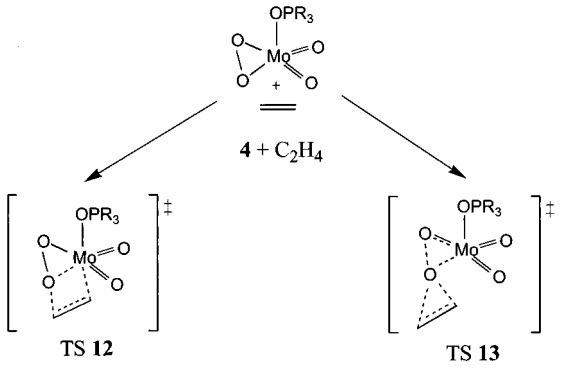

Table 2. Calculated Relative Energies E_{rel} (B3LYP/III+//B3LYP/II) [kcal/mol] for the Transition States of Ethylene Epoxidation with the Monoperoxo Complex $[MoO_2(O_2)(OPH_3)]$ (**4**) with ZPE-Corrected Values (B3LYP/II) Given in Parentheses

molecule/transition state		E_{rel}
$[MoO_2(O_2)(OPH_3)] + C_2H_4$	**4** + C_2H_4	0.0 (0.0)
TS direct cycloinsertion	TS **12a**	24.1 (26.3)
	TS **12b**	25.6 (27.4)
	TS **12c**	27.0 (29.2)
TS direct oxirane formation	TS **13a**	17.0 (17.8)
	TS **13b**	17.0 (18.0)

acetaldehyde from **3a** has an activation barrier via **TS11a** of 19.4 kcal/mol relative to **3a** (16.9 kcal/mol relative to **1** + C_2H_4). The Sharpless mechanism via **TS10a** leads to the correct product, i.e., the epoxide, with a barrier of only 15.2 kcal/mol.

We investigated theoretically whether the above conclusions will significantly change if the model ligand OPH_3 is substituted by the more realistic ligand $OPMe_3$. Table 1 shows the calculated energies of the relevant species. We only calculated those isomers and transition states which were found as the energetically lowest-lying forms in the parent system. The optimized geometries are shown as Supporting Information. The activation barrier for the Sharpless mechanism via **TS10aMe** is 17.5 kcal/mol, which is slightly higher than that for the parent compound. The activation barrier **TS8cMe** for the Mimoun mechanism is raised even more. Table 1 shows that the formation of the metalla-2,3-dioxolane has an activation energy of 28.4 kcal/mol. The extrusion reaction of **3aMe** leads again to acetaldehyde rather than ethylene oxide. It has a barrier of 19.3 kcal/mol relative to the starting material (18.0 kcal/mol relative to **3aMe**). The calculations suggest that the epoxidation of ethylene with $[Mo(O_2)_2OPR_3]$ does not take place via the Mimoun mechanism but via the Sharpless mechanism.

We investigated the question whether the monoperoxo complex **4** may also play a role in the epoxidation reaction. To this end we calculated the transition states which are relevant for the process shown in Scheme 5. The reaction step for binding ethylene to **4** needs not to be considered, because it was previously found that **4** does not bind ethylene.[29] Table 2 shows the calculated energies of the transition states **TS12** and **TS13**. The optimized geometries are given as Supporting Information. Three transition states **TS12a**−**TS12c** were found for the reaction which leads to the metalla-2,3-dioxolane, and two transition states **TS13a** and **TS13b** were found for the pathway which directly leads to the epoxide. The energetically lowest-lying transition state for the latter process **TS13a** gives a barrier of 17.8 kcal/mol, which is significantly lower than that for **TS12a** (26.3 kcal/mol). The barrier for the epoxidation reaction

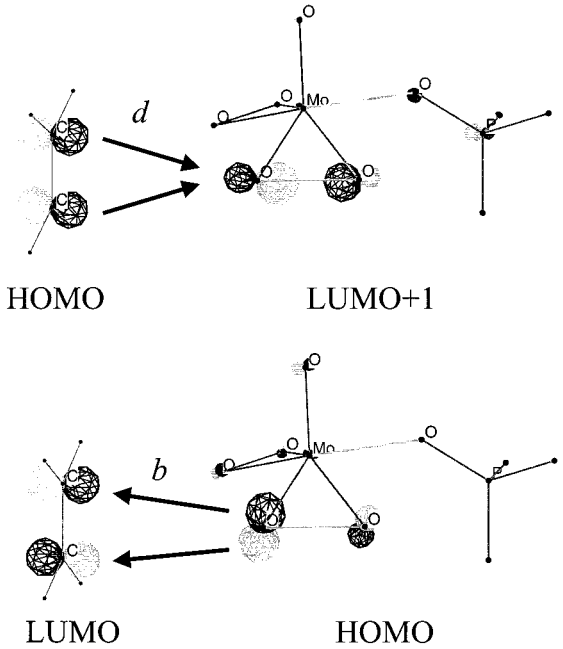

Figure 5. Plot of the dominant orbital interactions of the donation ethylene(HOMO) → [Mo](LUMO+1) and back-donation ethylene-(LUMO) ← [Mo](HOMO).

using the monoperoxo complex **4** (17.8 kcal/mol) is higher, however, than the barrier for epoxidation using the diperoxo complex (15.2 kcal/mol). The higher activation barrier of the former reaction is in agreement with experimental studies which showed that the diperoxo complexes but not the monoperoxo complexes of rhenium[45] and molybdenum[9] are active oxidants in epoxidation reactions. However, the energy difference of 2.6 kcal/mol between the transition states is not very big and it is conceivable that monoperoxo complexes might be used as the epoxidation agent under appropriate conditions.

We analyzed the electronic structure of the transition state for the epoxide formation of **TS10a** with the CDA method[39] to address the question whether the reaction is a nucleophilic attack of ethylene to the O−O bond or whether it is rather a nucleophilic attack of the peroxo group to ethylene. The latter mechanism of the electronic rearrangement has recently been suggested in a theoretical work at the EHT level.[18c] The CDA results of **TS10a** predict that the charge donation C_2H_4 → [Mo], where [Mo] denotes the diperoxo complex, is 0.233 e. The largest contribution comes from the donation of the HOMO of ethylene into the LUMO+1 of [Mo] (Figure 5). The back-donation C_2H_4 ← [Mo] is only 0.116 e, and the largest contribution comes from the HOMO of [Mo] and the LUMO of ethylene shown in Figure 5b. The value for the rest term was −0.005 e, which indicates that the interaction between ethylene and the diperoxo complex can be described in terms of donor−acceptor interactions.[40] The much larger charge donation from ethylene to the metal diperoxo complex suggests that the epoxidation reaction should be considered as a nucleophilic attack of ethylene toward the σ^*(O−O) bond, and not as a nucleophilic attack of the peroxo group to ethylene as proposed by EHT calculations.[18c]

The understanding of the nature of the electronic interaction in the transition state of the epoxidation reaction is not just a topic of academic interest. It also gives a hint about the factors which influence the height of the activation barrier. For example, the CDA result is in agreement with the theoretical finding that the substitution of OPH_3 by $OPMe_3$ increases the activation energy, because $OPMe_3$ enhances the electronic charge at the

diperoxo complex. It also explains why additional ligands L such as H_2O in $[MoO(O_2)_2(OPR_3)L]$ inhibit the transfer of an oxygen atom to the olefin. Mimoun originally proposed that the ligand L blocks the coordination of an olefin ligand and thus inhibits the epoxidation reaction.[10b] The present results support the interpretation of experimental findings[9] that the additional ligand L leads to a higher electronic charge at the reaction center which weakens its electrophilic character.

Summary and Conclusion

The theoretically predicted energies of the transition states and the calculated intrinsic reaction coordinates show that the epoxidation of olefins with molybdenum diperoxo complexes $[MoO(O_2)_2OPR_3]$ takes place in a single-step reaction via a direct attack of the olefin to the peroxo group as proposed by Sharpless. The alternative multiple-step reaction suggested by Mimoun can be ruled out. The metalla-2,3-dioxolane is only accessible via a direct reaction of the diperoxo complex and ethylene. The activation barrier for the formation of the intermediate is higher, however, than the activation barrier of the Sharpless mechanism. More important is the result that the decomposition reaction of the metalla-2,3-dioxolane leads to acetaldehyde and not to the epoxide. The monoperoxo complex $[MoO_2(O_2)OPR_3]$ has a higher activation barrier for the epoxidation reaction than the diperoxo complex, which is in agreement with experimental findings. Analysis of the electronic structure by Charge Decomposition Analysis of **TS10a** (the single transition state for the Sharpless mechanism) indicates that the epoxidation with metalla peroxides should be considered as a nucleophilic attack of ethylene toward the σ^* orbital of the O−O bond.

Acknowledgment. This work was supported by the Deutsche Forschungsgemeinschaft (SFB 260, Graduiertenkolleg Metallorganische Chemie and Schwerpunktprogramm Peroxidchemie) and by the Fonds der Chemischen Industrie. D.V.D. thanks the Fonds der Chemischen Industrie for a Kekulé-Stipendium. Excellent service by the Hochschulrechenzentrum of the Philipps-Universität Marburg is gratefully acknowledged. Additional computer time was provided by the HLRS Stuttgart, HHLRZ Darmstadt, and HRZ Frankfurt.

Supporting Information Available: Table of relative energies and a figure giving optimized energy minima (PDF). This material is available free of charge via the Internet at http://pubs.acs.org.

JA0006649